

# The Novaya Zemlya effect: An arctic mirage

W. H. Lehn

Department of Electrical Engineering, University of Manitoba, Winnipeg, R3T 2N2 Canada

(Received 13 September 1978)

The arctic mirage is an atmospheric refraction phenomenon caused by a temperature inversion in the lower atmosphere. It is classified into three basic types, two of which (*hillingar* and *hafgerdingar* effects) occur fairly frequently. The third is the Novaya Zemlya effect, reported by polar explorers on several occasions as an anomalous sunrise during the polar winter, when the position of the sun was below the horizon. The Novaya Zemlya effect consists of the trapping of light rays beneath a thermocline of large horizontal extent. Within the thermocline layers, the coefficient of refraction must exceed 1, while above and below it the coefficient must be less than 1. Then certain upward rays repeatedly bounce back from the thermocline and are transmitted for long distances around the earth's curvature. The anomalous sunrise is a special case of this generalized definition. The properties of the Novaya Zemlya effect, analyzed using a laterally uniform stratified-atmosphere model, agree with those reported by polar expeditions. A narrow strip or window appears near the horizon, with or without an image of the sun in the window. An observation sketched by Liljequist in Antarctica is reconstructed to demonstrate the model's accuracy.

## I. INTRODUCTION

The Novaya Zemlya effect is an atmospheric refraction phenomenon that is occasionally seen over large flat areas of the earth's surface. The effect consists of the trapping of light rays within the lowest layers of the atmosphere, by which process light can be transmitted for hundreds of kilometers around the curvature of the earth. The form in which it has been reported occurs when some direct rays from the sun are trapped so that an image of the sun appears, even though the sun is well below the horizon.

The effect is so named because it was first observed on the arctic island of Novaya Zemlya. In 1596 Captain Willem Barentz, leading his third polar expedition in search of the North-East Passage, got no farther than this island, where he was forced to spend the winter at a latitude of  $76^{\circ}12' N$ . On 24 January 1597, Gerrit de Veer, who accompanied Barentz, recorded in his journal that he and two shipmates observed the first return of the sun, a good two weeks earlier than its predicted return for that latitude.<sup>1</sup> At the time of this observation, the true solar altitude was  $-4.9^{\circ}$  (Fig. 1).<sup>2</sup> Three days later the sun again made an appearance, this time witnessed by many of the crew. The accuracy of De Veer's reported sightings was questioned by both his contemporaries and also by later scientists. However Kepler, as early as 1604, accepted the possibility of such sightings and attempted a scientific explanation.<sup>2</sup>

A more recent observation was made by Shackleton<sup>3</sup> during his last expedition to Antarctica (1914-17). In his account he described a reappearance of the sun on 8 May 1915, seven days after its final setting for the polar winter. The true solar altitude was  $-2^{\circ}37'$  at the time of this observation. A similar observation was made on 26 July 1915 (five days before the sun's scheduled return), when the solar altitude was about  $-2^{\circ}$ . Shackleton also described several appearances of thin black lines along the horizon. These were seen at times of winter twilight, once with "a small patch of the sun . . . thrown up on one of the black streaks." As Visser<sup>2</sup> correctly states, these sun sightings are observations of the Novaya Zemlya effect.

Several attempts at analysis have also been made. Wegener<sup>4</sup> constructed an internal-reflection model based on a temperature discontinuity in a stratified atmosphere. Basically, he explained what is known today as the ducting phenomenon of microwave transmission. However, his application to observations of distorted sunsets is valid only for short-range effects, and is incorrect for ranges characteristic of the Novaya Zemlya effect. Pernter and Exner<sup>5</sup> derived equations for anomalous astronomical refraction, but did not discuss long-range imaging; rather, they analyzed distorted sunsets by means of Wegener's short-range theory. Liljequist,<sup>6</sup> of whose observations more will be said later, saw several instances of the effect in Antarctica, just as powerful as that seen by Barentz. Liljequist applied Wegener's theory more correctly, in a descriptive kind of way, to explain his observations. Finally, Visser,<sup>2</sup> who at the time did not have access to Liljequist's observations, demonstrated from observed strengths of temperature inversions, that Barentz's observations had indeed not been a fabrication.

Neither Liljequist nor Visser attempted to analyze theoretically the shape of the observed image. Wegener, as well as Pernter and Exner, did concern themselves with imaging, but their explanations are not applicable to a true Novaya Zemlya effect.

The following sections classify atmospheric refraction into a few basic types, then describe in detail the conditions that produce the Novaya Zemlya effect, and the shape of the image

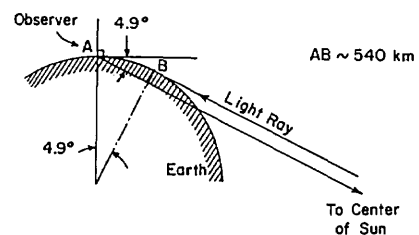


FIG. 1. Geometry of Barentz's observation. The ray to the sun's center is tangent to the earth at B, 540 km from the observer. From B to A, the atmosphere refracts rays around the earth's curvature.

that results. As an example, an image sketched by Liljequist is reconstructed with the aid of a computer.

## II. CLASSIFICATION OF REFRACTION TYPES

Refraction in the lower atmosphere can produce several types of images. First of all, the basic nature of the temperature profile establishes what kind of mirage will occur. If temperature decreases more rapidly than normal with elevation, the desert mirage results; if a temperature inversion exists, the arctic mirage occurs.<sup>7</sup> The latter has been variously named loom, superrefraction, and superior mirage.

The arctic mirage is here classified into three distinct types. The first two, for which the Icelandic words are used, are described in some detail in Refs. 7-9.

**A. Hillingar effect:** A mild atmospheric refraction, which makes the earth appear flat or saucer shaped. The effect is generated by a mild temperature inversion that is uniform over large distances. Nearly horizontal light rays are bent into arcs whose radii of curvature nearly equal that of the earth (Fig. 2). In other words, the refraction coefficient (see Appendix) is near unity.

**B. Hafgerdingar effect:** A strong nonuniform refraction, under which the earth's surface appears irregular, with vertical discontinuities. The Icelandic word, meaning "sea-fences", describes very well the visual impact. Multiple images of single objects may also appear. The temperature inversion that generates this effect is irregular, and the radius of curvature of the light rays varies widely with altitude (Fig. 3). The refraction coefficient  $k$  for many rays significantly exceeds unity.

**C. Novaya Zemlya effect:** In this case, the atmosphere possesses a strongly refracting layer ( $k > 1$ ) localized around some particular elevation, with weaker refraction ( $k < 1$ ) above and below this layer. The strong refraction occurs at a thermocline, returning certain rays to earth in a manner not unlike that of total internal reflection (Fig. 4). These rays are trapped and proceed around the earth's curvature until such a point where the refraction weakens enough that the rays can escape. To the eye, the trapped rays produce a narrow horizontal "window" in the atmosphere, through which light can travel for hundreds of kilometers. This definition is generalized to the extent that it is not necessary to have the sun appear in the window.

The following sections deal specifically with the characteristics of the Novaya Zemlya effect.

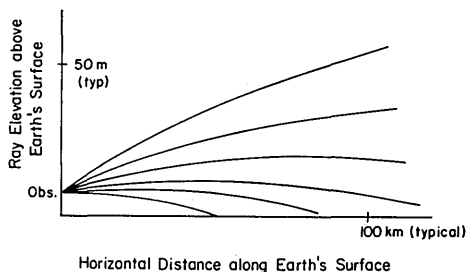


FIG. 2. Typical ray paths for the *hillingar* effect.

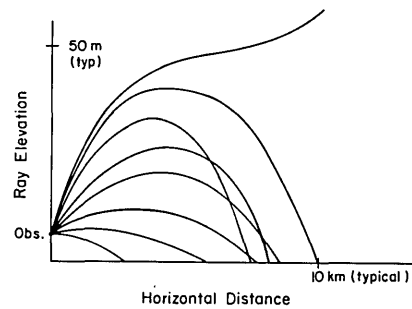


FIG. 3. Typical ray paths for the *hafgerdingar* effect.

## III. PROPERTIES OF THE NOVAYA ZEMLYA EFFECT

The general propagation of light rays through the lower atmosphere has been described in detail in Refs. 8 and 10.

A few basic necessities suffice to produce the effect. The atmosphere must possess a temperature inversion with a thermocline. Above and below the thermocline, the atmosphere can have almost any properties, as long as the coefficient of refraction  $k$  is less than one. The thermocline, on the other hand, must produce refraction strong enough ( $k > 1$ ) to return toward the earth all rays travelling upward at angles below some specific value. Further, most of the returning rays must not intersect the earth: they must have earth-grazing paths which (due to curvature of the earth) ultimately head upwards, only to be returned again from the thermocline. The effect can develop properly only over flat featureless terrain, for only over such landscape can the same temperature inversion exist over a sufficiently large area. The necessary temperature conditions are not in themselves extreme; for example, an inversion of magnitude  $6^\circ\text{C}$  with maximum temperature gradient of  $0.2^\circ\text{C}/\text{m}$  is quite adequate. The most difficult of the conditions to be met is the vast uniform expanse of atmosphere, with inversion everywhere the same.

The appearance of the effect is that of a thin horizontal gray band near the horizon. This band is in reality a "window", through which the observer is seeing objects many times farther away than normal lines of sight. Above and below the window, objects at normal distances are seen. The window can be above, on, or below the normal horizon. The grayness of the window (it is darker than the regions above and below it) arises from atmospheric absorption.

Some of the more detailed physical and optical properties of the Novaya Zemlya effect will now be described. Some of

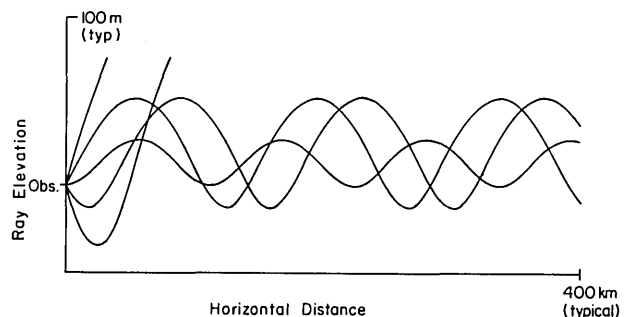


FIG. 4. Typical ray paths for the Novaya Zemlya effect.

the main features are shown in Fig. 4. Rays with certain initial angles  $\phi_0$  are trapped below the thermocline. These initial angles lie within a range symmetrical about  $\phi_0 = 0^\circ$  i.e.,  $|\phi_0| \leq \phi_m$ . The observer thus sees a window of vertical extent  $[-\phi_m, \phi_m]$ . The limiting angle  $\phi_m$  is a function of observer height relative to the thermocline, with the widest windows arising when the observer is at about half the elevation of the thermocline. Rays with  $\phi_0$  outside the interval  $[-\phi_m, \phi_m]$  have only a short "local" range: They either intersect the ground or head off into space, at relatively short distances from the observer.

The ray paths are periodic with respect to horizontal distance  $x$  measured along the earth's surface. This is a necessary consequence of the choice of atmospheric model, namely, a stratified atmosphere, homogeneous laterally, whose properties vary in a vertical direction only. The shape of a ray is then symmetrical about a vertical line drawn through any maximum or minimum. It follows that long rays, repeatedly returned from the thermocline, will possess equally spaced lines of symmetry, and hence will be periodic. It should be noted that symmetry does *not* extend so far as to make upper and lower half cycles identical in shape; the ray does not have half-wave symmetry.

The ray that begins horizontally ( $\phi_0 = 0$ ) has the shortest spatial period, as well as the smallest amplitude. This happens because, of all the rays, the  $\phi_0 = 0$  ray meets the thermocline region with the shallowest angle, and is most easily returned to earth. As  $\phi_0$  deviates from zero either positively or negatively, the spatial periods and amplitudes increase. There is symmetry with respect to the sign of  $\phi_0$ : The ray for a given  $\phi_0$  is identical in shape to that for  $-\phi_0$ ; there is only a phase shift (shift in horizontal position).

Image transmission through the window by these trapped rays would proceed in a very orderly manner if all the rays had the same period. Then  $\phi_0$  would control only the phase; if a ray (starting at the observer's eye) meets an object while the ray is on its return from the thermocline, this object would appear inverted; if the object were intersected by rays heading upward, it would appear erect (within the window). Unfortunately such a simple analysis is not valid in the actual case. Because different values of  $\phi_0$  produce rays with different periods, these rays accumulate lateral shift relative to each other, as they gain distance from the observer. Some image distortion can be demonstrated even after the first return from the thermocline. With each cycle the distortion gets worse, until finally the rays appear to occupy a completely random pattern. After a few cycles, most identifiable image details are distorted beyond recognition.

#### IV. COMPUTATION OF IMAGES

From his station in Maudheim, Antarctica, Liljequist observed and sketched several cases of the Novaya Zemlya effect. One of these sketches (Fig. 8 of Ref. 6) is reproduced in Fig. 5. This observation was made on 1 July 1951, at a time when the true solar altitude at the station (latitude  $71^\circ 03'S$ ) was  $-4.3^\circ$ . Temperature readings made within a few hours showed a very strong inversion, of total strength  $25^\circ C$ , extending up to 1000 m elevation. However, the spacing of the readings at the critical low-elevation layers was too great to identify any low-level thermocline.

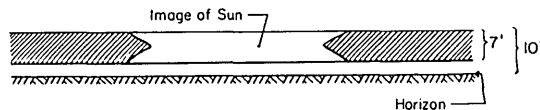


FIG. 5. Liljequist's sketch of the Novaya Zemlya effect, July 1, 1951 (Ref. 6). "The sun was seen like a red and partly bipartite strip, situated wholly within a relatively dark horizontal strip of the same breadth and with its lower rim about 3' above the ice-shelf horizon."

Wegener's theory of atmospheric reflections, while remaining a reasonable approximation for short-range work, runs into difficulty when trying to explain the Novaya Zemlya effect. It does not account for rays breaking out of the "trapped" region and finally leaving the atmosphere. Wegener even gives an example of a distorted sunset, but in this case the window is blank with the sun appearing above and below it; whereas in the true Novaya Zemlya effect, the sun appears only *within* the window. Similarly, Liljequist and Visser do not address the breakout problem for the trapped rays.

The following paragraphs describe the reconstruction of Liljequist's observation (Fig. 5) on a theoretical basis. The general methods of image construction are treated in Refs. 8 and 10. A temperature profile is assumed for the atmosphere. Then a bundle of rays is computed, emanating from the observer's station. Many of the rays are trapped, up to the point where the thermocline ceases to exist, after which they are assumed to travel in almost straight lines through a nearly normal atmosphere. To construct the image, one must identify the initial angle  $\phi_0$  corresponding to each intersection of ray with object. The values of  $\phi_0$  determine what the eye sees ( $\phi_0$  is the ray angle as it enters the eye) since the eye assumes that all the light rays it perceives are straight lines.

The specific reconstruction of Fig. 5 is done in two stages: First, the correct width and elevation of the window are generated, then the correct shape of the sun. With Liljequist's temperature data as basis, several temperature profiles were tried. The profile of Fig. 6 generates the window correctly (a

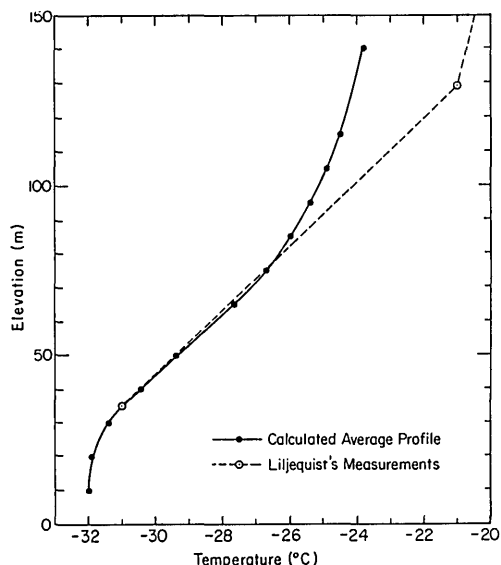


FIG. 6. Temperature profile required to reproduce Liljequist's observation.

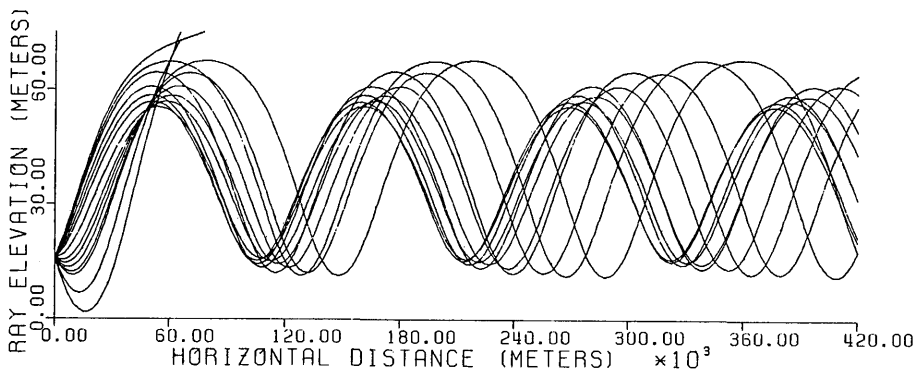


FIG. 7. Computer drawing of ray paths generated by the temperature profile of Fig. 6. The sequence of initial ray angles, starting with the uppermost ray, is  $0.06^\circ$ ,  $0.055^\circ$ ,  $0.05^\circ$ ,  $0.04^\circ$ ,  $0.03^\circ$ ,  $0.02^\circ$ ,  $0.0^\circ$ ,  $-0.02^\circ$ ,  $-0.03^\circ$ ,  $-0.04^\circ$ ,  $-0.05^\circ$ ,  $-0.055^\circ$ ,  $-0.08^\circ$ , and  $-0.10^\circ$ .

width of 7 min, with bottom edge 3 min above the horizon), although it does not pass precisely through Liljequist's data points. The discrepancy is not significant, because the measured data refer to temperatures at the station, whereas the ray-propagation program requires a temperature profile averaged over several hundred kilometers of path through the atmosphere. The observer's elevation in the reconstruction is taken to be 16 m above sea level—a not unreasonable estimate in the absence of reported data. It should be noted that no claim can be made for a unique identification of the correct temperature profile; there may well be slightly different profiles which, together with different observer elevations, produce windows of similar dimensions. Figure 7 shows the computed ray paths for the atmosphere of Fig. 6.

Next, the best fit to the observed *shape* of the sun is sought. The refracting atmosphere is assumed to revert to normal at various distances from the observer. Beyond this point, the rays are assumed to be straight (this assumption is corrected later for "normal" atmospheric refraction). The critical distance that best reproduces the notched image of the sun is 390 km.

At this distance, the angles of the rays with respect to the horizontal are calculated, and the rays are projected out into space. This ray bundle does not meet the sun when  $h =$

$-4.3^\circ$ . However, there is further refraction to account for, which will be assumed to be slightly higher than normal due to the extremely cold air present at the time. Whereas standard astronomical refraction<sup>4</sup> for a horizontal ray is  $35'$  or  $0.58^\circ$ , the best image match is achieved for the slightly higher value of  $0.91^\circ$ .

Further, there is some ray divergence which should be accounted for as the rays proceed out of the atmosphere beyond the 390 km distance. Refraction values for the normal atmosphere are used to estimate this divergence, as follows. The rays leaving the abnormal atmosphere at 390 km have angles in the approximate range  $\pm 5'$  relative to the local horizontal. Now, while the normal atmosphere refracts a level ray downward by  $35'$  before it leaves the atmosphere, it refracts a ray with  $\phi_0 = +5'$  by only  $34'$ , but a ray with  $\phi_0 = -5'$  by  $36'$ . Hence rays with  $\phi_0 = \pm 5'$  which initially diverge by  $10'$ , end up diverging by  $10' + 2' = 12'$  as they leave the atmosphere. It follows that ray angles calculated at 390 km must be multiplied by  $12/10 = 1.2$  to yield relative ray angles outside the atmosphere. Figure 8 shows the resulting mapping that relates  $\phi_0$  to relative ray angle ( $\phi_{390}$ ) leaving the atmosphere.

The above approximate corrections for events beyond 390 km are deemed sufficiently accurate for the purpose at hand—namely, to generate an image of the sun. These assumptions are no more severe than the assumption of a uniform anomalous atmosphere over a 390 km space.

The sun can occupy any position relative to the  $\phi_{390}$  rays. The best match occurs when the  $\phi_{390} = 0^\circ$  ray intersects the

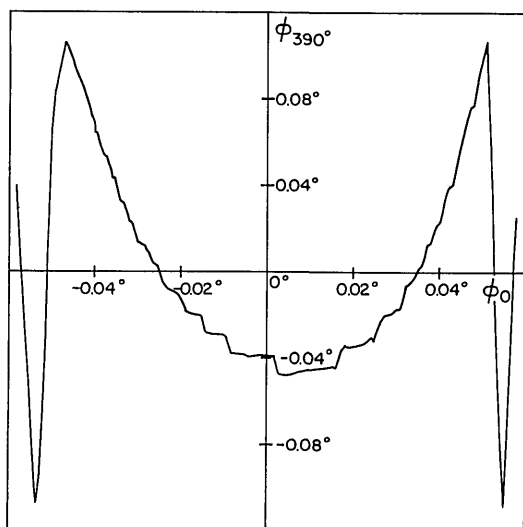


FIG. 8. Mapping of ray angle at 390 km vs ray angle at observer's eye, for the temperature profile of Fig. 6.

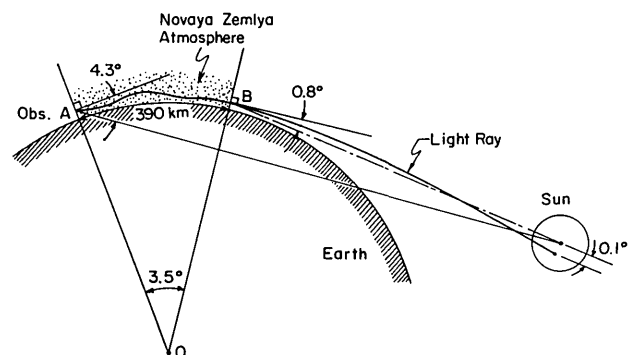


FIG. 9. Configuration producing the best reconstruction of Liljequist's observation.

TABLE I. Typical values for  $k$  based on different temperatures and temperature gradients. The pressure is taken as the normal earth-surface value:  $1.013 \times 10^5 \text{ nm}^{-2}$ .

Temperature gradient ( $^{\circ}\text{K/m}$ )	Temperature ( $^{\circ}\text{K}$ )				
	233	253	273	293	313
-.006	0.26	0.22	0.19	0.17	0.15
0	0.32	0.27	0.23	0.20	0.18
.073	1.00	0.85	0.73	0.64	0.56
.112	1.37	1.16	1.00	0.87	0.76
.2	2.19	1.86	1.60	1.39	1.22

sun  $0.10^{\circ}$  below the sun's center (Fig. 9). The corresponding calculated image of the sun is shown in Fig. 10. Within the accuracy of Liljequist's sketch, the agreement between calculated image and observed image is complete.

The fine structure at the edges of the calculated image requires some comment. In practice it can be ignored. In all likelihood it would not be observed unless the observer was specifically looking for it. Further, it would be the first feature to be obliterated by the slightest irregularity in the air layers containing the thermocline.

The darkness or "grayness" of the window is due to atmospheric absorption of light. After passing through hundreds of kilometers of air, no matter how dry and pollution free, light loses most of its energy. A ray will possess only a few percent of its initial energy,<sup>8</sup> allowing the eye to look directly at the sun image. The rest of the window is rendered very dark, for in this zone the *only* light reaching the eye is that which has hundreds of kilometers' absorption behind it. Shackleton's unexplained black streaks on the horizon are most likely Novaya Zemlya windows without the sun's appearance within them.

It should be noted that the images of Figs. 5 and 10 are not the only ones possible with the Novaya Zemlya effect. The image of the sun need not fill the window. Depending on the position of the sun relative to the ray bundle emanating from the abnormal atmosphere, the sun could appear as two narrow strips, at the top and bottom edges of the window respectively; or even as three strips of possibly different widths, one above the other. Similarly, terrestrial objects could appear in the window (e.g., a distant coastline), but in this case the dimness and distortion of the image would make recognition difficult.

## V. CONCLUSION

The three distinct manifestations of the arctic mirage have been classified. The *hillingar* and *hafgerdingar* effects are common; they can be seen almost any time over large bodies of water by an observant person. The Novaya Zemlya effect,

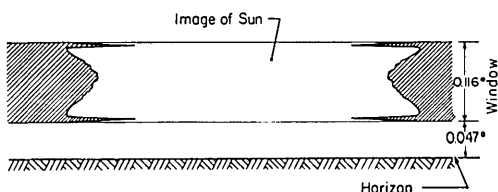


FIG. 10. Calculated appearance of sun (cf. Fig. 5.)

on the other hand, is a rarely reported but extremely impressive optical effect. Observations to date have been restricted to the polar regions largely because the reappearance of the sun during the winter night is such an obvious event. Flat polar regions in winter offer ideal conditions for generating the necessary uniform widespread temperature inversion. The scarcity of reports is due to the fact that the effect is recognized only when the sun occupies just the right position for it to appear in this way.

The definition of the Novaya Zemlya effect has been generalized to include all phenomena that involve the trapping of light rays. With the revised definition the effect would be observed more widely, for example over high-latitude seas under a stable temperature inversion. The necessary temperature conditions are not extreme; the critical factors are the uniformity of air and earth's surface over very large distances.

## APPENDIX

The coefficient of refraction  $k$  of the atmosphere is defined as

$$k = \frac{\text{radius of the earth}}{\text{radius of curvature of light ray}}.$$

An equation relating  $k$  to atmospheric parameters can be derived from the equations that appear in Ref. 8.

The refractive index of air is given by

$$n = 1 + \epsilon\rho, \quad (1)$$

where  $\rho$  is air density ( $\text{kgm}^{-3}$ ) and  $\epsilon = 226 \times 10^{-6}$ . Density is related to pressure  $p$  ( $\text{nm}^{-2}$ ) and temperature  $T$  ( $^{\circ}\text{K}$ ) by

$$\rho = \beta(p/T), \quad (2)$$

where the constant of proportionality is  $\beta = 3.49 \times 10^{-3}$ . For a given temperature profile  $T(z)$ , the variation of pressure with elevation  $z$  is given by

$$p = p_0 e^{-g\beta \int_0^z [dz'/T(z')]}, \quad (3)$$

where  $g = 9.8 \text{ ms}^{-2}$ , and subscript "0" refers to surface values.

Finally, the radius of curvature  $r$  of nearly level light rays is found from

$$\frac{1}{r} = \frac{\epsilon}{1 + \epsilon\rho} \frac{d\rho}{dz}. \quad (4)$$

Equations (1)–(4) are combined to yield an expression for the coefficient of refraction:

$$k = \frac{R\epsilon\beta\rho}{(1 + \epsilon\rho)T^2} \left( \frac{dT}{dz} + g\beta \right). \quad (5)$$

In this formula,  $R$  is the radius of the earth ( $6.37 \times 10^6$ m). A positive result for  $k$  implies that the ray is concave toward the earth (center of curvature is on the earthward side of the ray). See Table I.

- <sup>1</sup>G. deVeer, *The Three Voyages of William Barents to the Arctic Regions (1594, 1595 and 1596)*, 2nd ed. (Hakluyt Society, London, 1876).  
<sup>2</sup>S. W. Visser, "The Novaya-Zemlya Phenomenon," *K. Ned. Akad. Wet. Versl. Gewone Vergad. Afd. Natuurkd.* 59, 375-385 (1956).  
<sup>3</sup>E. Shackleton, *South-The Story of Shackleton's Last Expedition*

- 1914-1917, (MacMillan, New York, 1920).  
<sup>4</sup>A. Wegener, "Elementare Theorie der atmosphärischen Spiegelungen," *Ann. Phys. (Leipzig)* 57, 203-230 (1918).  
<sup>5</sup>J. M. Pernter and F. M. Exner, *Meteorologische Optik*, 2nd ed. (Braumüller, Vienna, 1922).  
<sup>6</sup>G. H. Liljequist, "Refraction Phenomena in the Polar Atmosphere," in *Scientific Results, Norwegian-British-Swedish Antarctic Expedition, 1949-52*, Vol. 2, Part 2, (Oslo University, Oslo, 1964).  
<sup>7</sup>H. L. Sawatzky and W. H. Lehn, "The Arctic Mirage and the Early North Atlantic," *Science*, 192, 1300-1305 (1976).  
<sup>8</sup>W. H. Lehn and H. L. Sawatzky, "Image Transmission under Arctic Mirage Conditions," *Z. Polarforschung*, 45, 120-128 (1975).  
<sup>9</sup>W. H. Lehn, H. L. Sawatzky *et al.*, "Lore, Logic and the Arctic Mirage", *Scand. Review*, 66, 36-41 (1978).  
<sup>10</sup>W. H. Lehn and M. B. El-Arini, "Computer-graphics analysis of atmospheric refraction", *Appl. Opt.*, 17, 3146-3151 (1978).

## Analysis of resonant Voigt effect

Manabu Yamamoto and Seiichi Murayama

Central Research Laboratory, Hitachi, Ltd., Kokubunji, Tokyo 185, Japan

(Received 1 November 1978)

An analysis that expands the resonant Voigt effect theory is presented. Elliptically polarized incident light interacts with atoms of a general Zeeman structure. The atoms are subjected to an externally applied transverse magnetic field. Light scattered in the forward direction is analyzed as to polarization. Under these conditions, light intensity transmitted by the polarization analyzer is calculated as a function of frequency and ellipticity of the incident light, atomic number density, and analyzer orientation. An experiment on forward scattering of circularly polarized light is also presented. This technique offers an alternative method of trace-element determination.

### I. INTRODUCTION

The resonant Voigt effect, or magnetically induced birefringence for resonance radiation, takes place when incident light is scattered by atoms subjected to an externally applied transverse magnetic field. The resonant magneto-optic effect, both in a transverse and in a longitudinal field, has been investigated extensively.<sup>1</sup> In principle, the effect can be described in terms of three basic functions: the birefringence function, the Faraday function, and the mean dispersion function. Explicit forms for these functions have previously been given for the transition of a simple Zeeman structure.

Experiments to date have been performed under the condition that the scattering vapor is placed between a crossed polarizer and analyzer. With this configuration, atoms are irradiated by linearly polarized light, and light scattered by the atoms in the forward direction is analyzed as to polarization. The polarization analyzer is oriented in a direction orthogonal to the incident-light polarization.

However, the resonant magneto-optic effect has recently proved to be useful in trace element detection,<sup>2,3,4</sup> thereby creating a need for a broader formulation of the theory. In view of this necessity for further development of magneto-optic techniques, an analysis which expands the resonant Voigt effect theory is presented here. The basic assumptions are as follows: (i) the incident light is polarized elliptically, (ii) the scattering atoms have a general Zeeman structure, (iii) the polarization analyzer may be oriented in any direction with

respect to the magnetic field. Under these conditions, the light intensity transmitted by the analyzer is calculated as a function of the frequency and ellipticity of the incident light, the atomic number density, and the analyzer orientation.

### II. CALCULATION OF FORWARD-SCATTERED LIGHT INTENSITY

With the magnetization direction parallel to the  $z$  axis, the dielectric tensor of a medium is given by<sup>5</sup>

$$\| \epsilon_{ij} \| = \begin{bmatrix} \epsilon_e & \epsilon' & 0 \\ -\epsilon' & \epsilon_e & 0 \\ 0 & 0 & \epsilon_o \end{bmatrix}. \quad (1)$$

When light is propagated along the  $x$  axis, the indices of refraction for the normal modes are

$$n_e = [(\epsilon_e^2 + \epsilon'^2)/\epsilon_e]^{1/2} \simeq \sqrt{\epsilon_e},$$

$$n_o = \sqrt{\epsilon_o}, \quad (2)$$

where indices  $o$  and  $e$  represent ordinary and extraordinary waves respectively. A wave propagating in the medium is described as follows:

$$\mathbf{E} = (E/\sqrt{2})[\mathbf{j} \exp(ikn_e x) e^{-i\alpha} + \mathbf{k} \exp(ikn_o x) e^{i\alpha}] \exp(-i\omega t). \quad (3)$$

In the above equation,  $E$  is the light wave amplitude,  $\mathbf{j}$  and  $\mathbf{k}$  are unit vectors in the  $y$ - and  $z$ -directions respectively,  $\omega$  is